

Designable Coordination Bonding in Mesopores
as a pH-Responsive Release SystemChuanbo Gao,[†] Haoquan Zheng,[†] Lei Xing,[†] Mouhai Shu, and Shunai Che**School of Chemistry and Chemical Engineering, State Key Laboratory of Metal Matrix Composites, Shanghai Jiao Tong University, Key Laboratory for Thin Film and Microfabrication Technology of the Ministry of Education, 800 Dongchuan Road, Shanghai 200240, People's Republic of China.*[†]These authors have contributed equally to this work.

Received March 4, 2010. Revised Manuscript Received July 26, 2010

pH-responsive systems are promising in their applicability to many areas, e.g., in drug delivery. Herein, we report a novel versatile pH-responsive system based on the coordination bonding of metal ions and functional groups in mesopores. Organic group functionalized mesoporous silica nanoparticles were employed as typical carriers for hosting metal ion binders and guest molecules to form a “host–metal–guest” architecture. The cleavage of either the “host–metal” or the “metal–guest” coordination bond, in response to pH variations, gives rise to a significant release of guest molecules under designated pH conditions. Using amino group functionalized mesoporous silica and choosing proper metal ions, the successful release of anticancer drugs bearing coordination binding groups was achieved at pH 5.0–6.5. Furthermore, a vector bearing pH-responsive binding functional groups is designed to assist in the release of drugs without significant binding capabilities. This route opens up a facile but powerful avenue for the design of various pH-responsive systems and new opportunities for their application in drug delivery.

Stimuli-responsive systems provide a variety of promising applications in biomedical fields,^{1,2} and these “smart” systems have attracted the interest of a broad range of researchers in recent years. Diverse physical forms of such systems have been developed to date, including hydrogels,^{3,4}

micelles,^{5–7} liposomes,^{6,8–11} inorganic solids,^{12–29} etc. These systems take up or release guest molecules in response to external stimuli such as temperature,^{4,24} pH,^{3–23} light irradiation,^{4,25–27} ionic strength,^{13,14} redox reagents,²⁸ enzymes,²⁹ etc. All these methods pave the way for precise spatial and temporal delivery of guest molecules to target sites. Of these stimuli-responsive systems, the pH-sensitive system is of special interest.³⁰ The extracellular pH of tumors is more acidic (pH 5.7–7.8) than that of blood and normal tissue,³¹ and the pH values in endosomes and

*Author to whom correspondence should be addressed. Tel.: +86-21-5474-2852. Fax: +86-21-5474-1297. E-mail: chesa@sjtu.edu.cn.

- (1) Gil, E. S.; Hudson, S. M. *Prog. Polym. Sci.* **2004**, *29*, 1173–1222.
- (2) de las Heras Alarcón, C.; Pennadam, S.; Alexander, C. *Chem. Soc. Rev.* **2005**, *34*, 279–285.
- (3) Gupta, P.; Vermani, K.; Garg, S. *Drug Discovery Today* **2002**, *7*, 569–579.
- (4) Qiu, Y.; Park, K. *Adv. Drug Delivery Rev.* **2001**, *53*, 321–339.
- (5) Taillefer, J.; Jones, M.-C.; Brasseur, N.; van Lier, J. E.; Leroux, J.-C. *J. Pharm. Sci.* **2000**, *89*, 52–62.
- (6) Leroux, J.-C.; Roux, E.; Garrec, D. L.; Hong, K.; Drummond, D. C. *J. Controlled Release* **2001**, *72*, 71–84.
- (7) Gillies, E. R.; Fréchet, J. M. J. *Chem. Commun.* **2003**, 1640–1641.
- (8) Yatvin, M. B.; Kreutz, W.; Horwitz, B. A.; Shinitzky, M. *Science* **1980**, *210*, 1253–1255.
- (9) Drummond, D. C.; Zignani, M.; Leroux, J.-C. *Prog. Lipid Res.* **2000**, *39*, 409–460.
- (10) Guo, X.; Szoka, F. C., Jr. *Acc. Chem. Res.* **2003**, *36*, 335–341.
- (11) Lee, S.-M.; Chen, H.; Dettmer, C. M.; O'Halloran, T. V.; Nguyen, S. T. *J. Am. Chem. Soc.* **2007**, *129*, 15096–15097.
- (12) Casasús, R.; Marcos, M. D.; Martínez-Mañez, R.; Ros-Lis, J. V.; Soto, J.; Villacusa, L. A.; Amorós, P.; Beltrán, D.; Guillem, C.; Latorre, J. J. *Am. Chem. Soc.* **2004**, *126*, 8612–8613.
- (13) Casasús, R.; Climent, E.; Marcos, M. D.; Martínez-Mañez, R.; Sancenón, F.; Soto, J.; Amorós, P.; Cano, J.; Ruiz, E. *J. Am. Chem. Soc.* **2008**, *130*, 1903–1917.
- (14) Zhu, Y.; Shi, J.; Shen, W.; Dong, X.; Feng, J.; Ruan, M.; Li, Y. *Angew. Chem., Int. Ed.* **2005**, *44*, 5083–5087.
- (15) Yang, Q.; Wang, S.; Fan, P.; Wang, L.; Di, Y.; Lin, K.; Xiao, F.-S. *Chem. Mater.* **2005**, *17*, 5999–6003.
- (16) Song, S.-W.; Hidajat, K.; Kawi, S. *Chem. Commun.* **2007**, 4396–4398.
- (17) Wu, W.; Gao, Q.; Xu, Y.; Wu, D.; Sun, Y. *Mater. Res. Bull.* **2009**, *44*, 606–612.

- (18) Nguyen, T. D.; Leung, K. C.-F.; Liong, M.; Pentecost, C. D.; Stoddart, J. F.; Zink, J. I. *Org. Lett.* **2006**, *8*, 3363–3366.
- (19) Leung, K. C.-F.; Nguyen, T. D.; Stoddart, J. F.; Zink, J. I. *Chem. Mater.* **2006**, *18*, 5919–5928.
- (20) Angelos, S.; Yang, Y.-W.; Patel, K.; Stoddart, J. F.; Zink, J. I. *Angew. Chem., Int. Ed.* **2008**, *47*, 2222–2226.
- (21) Park, C.; Oh, K.; Lee, S. C.; Kim, C. *Angew. Chem., Int. Ed.* **2007**, *46*, 1455–1457.
- (22) Lee, C.-H.; Lo, L.-W.; Mou, C.-Y.; Yang, C.-S. *Adv. Funct. Mater.* **2008**, *18*, 3283–3292.
- (23) Wang, B.; Xu, C.; Xie, J.; Yang, Z.; Sun, S. *J. Am. Chem. Soc.* **2008**, *130*, 14436–14437.
- (24) Zhou, Z.; Zhu, S.; Zhang, D. *J. Mater. Chem.* **2007**, *17*, 2428–2433.
- (25) Mal, N. K.; Fujiwara, M.; Tanaka, Y.; Taguchi, T.; Matsukata, M. *Chem. Mater.* **2003**, *15*, 3385–3394.
- (26) Nguyen, T. D.; Leung, K. C.-F.; Liong, M.; Liu, Y.; Stoddart, J. F.; Zink, J. I. *Adv. Funct. Mater.* **2007**, *17*, 2101–2110.
- (27) Park, C.; Lee, K.; Kim, C. *Angew. Chem., Int. Ed.* **2009**, *48*, 1275–1278.
- (28) Lai, C.-Y.; Trewyn, B. G.; Jeftinija, D. M.; Jeftinija, K.; Xu, S.; Jeftinija, S.; Lin, V. S.-Y. *J. Am. Chem. Soc.* **2003**, *125*, 4451–4459.
- (29) Schlossbauer, A.; Kecht, J.; Bein, T. *Angew. Chem., Int. Ed.* **2009**, *48*, 3092–3095.
- (30) Leung, K. C.-F.; Chak, C.-P.; Lo, C.-M.; Wong, W.-Y.; Xuan, S.; Cheng, C. H. K. *Chem. Asian J.* **2009**, *4*, 364–381.
- (31) Engin, K.; Leeper, D. B.; Cater, J. R.; Thistlethwaite, A. J.; Tupchong, L.; McFarlane, J. D. *Int. J. Hypertherm.* **1995**, *11*, 211–216.

lysosomes reach values as low as 5.5 and 5.0, respectively.³² Therefore, a finely pH-responsive system, sensitive to small pH variations, that would release encapsulated drugs when passing through a region of low pH (pH 5–7) while staying stable under physiological conditions to reduce side effects, has been pursued for some time.

State-of-the-art pH-responsive systems based on soft matter and inorganic solids are categorized into several types. Common routes for soft matter systems include utilizing the dimensional changes of hydrogels triggered by a swelling/deswelling effect^{1–4} and the stabilization/destabilization of micelles and liposomes.^{5–11} Typical inorganic solid-based pH-responsive systems usually involve on/off capping or gating (by functional groups,^{12,13} polyelectrolytes,^{14–17} and ring-shaped compounds^{18–21}) or host–guest interactions (electrostatic²² and covalent bonding²³). For these methods to function, driving forces commonly changes in the electrostatic state, polarity, hydrophobicity, or conformation of the pH-sensitive polymers, surfactants, or anchored functional groups, as a result of hydrolysis or a change in ionization under different pH conditions. However, a finely responsive system that would release guest molecules by small pH variations has been pursued for a long time and remains a challenge.

Herein, we represent a mesoporous-silica pH-responsive release system based on the pH sensitivity of the formation and cleavage of coordination bonding between metal ions and functional groups. The formation and cleavage of metal ion–ligand coordination bonds are sensitive to external pH variations, because both metal ions and protons (H^+) are Lewis acids and compete to combine with the ligand, which is a Lewis base. Therefore, it is possible to use coordination bonding to realize a pH-responsive release system. This mechanism can be found in nature, e.g., in the transferrin recycling in cells.³³ Fe ions are transferred from the extracellular environment into the cytoplasm by the formation and breakage of coordination bonds in response to a pH change. Therefore, the pH-responsive strategy, using coordination bonding, is a biomimetic process. On the other hand, mesoporous silica material is a good carrier for constructing the pH-responsive release system on the basis of coordination–bonding not only because it provides space to host guest molecules and prevents them from chemical or biological attack by external substances before their intended release, but, more importantly, because it satisfies prerequisite conditions for the functioning of the coordinative pH response as described below, e.g., the coordination unsaturation of metal ions after being absorbed onto the mesopores for the loading of guest molecules.

Experimental Section

Chemicals. *N*-stearoyl-L-glutamic acid ($C_{18}GluA$) was synthesized following the procedure described in our earlier paper (also see the Supporting Information).³⁴ Fluorescein isothiocyanate–

octaarginine (FITC-R8) was prepared by Fmoc (9-fluorenylmethoxycarbonyl)–solid-phase peptide synthesis on a Rink amide resin, where γ -aminobutyric acid was employed as a spacer to connect FITC with the R8 segment.

The following reagents were purchased from Sinopharm and used without purification: tetraethyl orthosilicate (TEOS), $Cu(ClO_4)_2 \cdot 6H_2O$, $Cu(NO_3)_2 \cdot 3H_2O$, $Zn(NO_3)_2 \cdot 6H_2O$, $NH_4Fe(SO_4)_2 \cdot 6H_2O$, ethylene diamine, propylamine, diethylene triamine, and *o*-phenylene diamine. Other chemicals, including Pluronic P123 ($EO_{20}PO_{70}EO_{20}$, BASF), 3-aminopropyltrimethoxysilane (APS, TCI), 1,1-dimethylbiguanide (Sigma–Aldrich), phenformin (Sigma–Aldrich), mitoxantrone (MX, FINC), and daunorubicin hydrochloride (DNR, Meryer), were used as purchased.

Synthesis of Aminopropyl-Functionalized AMS Nanoparticles. Typically, 0.60 g of P123 was dissolved in 41.3 g of deionized water at room temperature, after which 0.413 g (1 mmol) of $C_{18}GluA$ was added and dispersed at 80 °C. Afterward, 0.358 g (2 mmol) of APS was added to the synthesis system, and 3.12 g (15 mmol) of TEOS was added after 30 s. The mol composition of the synthesis system was $C_{18}GluA:P123:APS:TEOS:H_2O = 1:0.103:2:15:2294$. The reaction mixture was stirred for 10 min and aged at 80 °C for 2 days. The precipitate was collected by centrifugation. The removal of surfactant from the as-synthesized AMS nanoparticles was achieved by extraction with ethanolic solution of ethanolamine.³⁵

Loading of Metal Ions into the Aminopropyl Functionalized AMS nanoparticles To Form “ NH_2 –Metal” Coordination Bonds. Stock solutions (1.0 mM) of Cu^{2+} , Zn^{2+} , and Fe^{3+} were prepared by dissolving $Cu(NO_3)_2 \cdot 3H_2O$, $Zn(NO_3)_2 \cdot 6H_2O$, and $NH_4Fe(SO_4)_2 \cdot 6H_2O$ in absolute ethanol, respectively. In a typical charging process of metal ions into the aminopropyl functionalized AMS nanoparticles, 0.15 g of AMS material was dispersed in 8 mL of the stock solution, and the mixture was stirred at ambient temperature for 2 h. The AMS materials were recovered by centrifugation, washed 10 times with ethanol, and dried at 40 °C overnight.

Loading of Guest Molecules into Metal–Ion Loaded AMS Nanoparticles To Form “ NH_2 –Metal–Guest” Coordination Bonds. Typically, 50 mg of metal-ion-loaded AMS nanoparticle material was dispersed in 8.0 mL of 0.1 mM solution of guest molecules at pH 7.4 and ambient temperature, and further stirred for 4 h. After that, the solid product was recovered by centrifugation, washed with water (pH 7.4) 10 times, and dried at 40 °C overnight.

Release of Guest Molecules under Different pH Conditions. In a typical release experiment, 6.0 mg of the AMS material with absorbed guest molecules was suspended by vibration in 25.0 mL of aqueous solution with various pH from 8.0 to 1.2, at 37 °C. For *o*-phenylenediamine and phenformin, the release medium was water with pH carefully tuned by NaOH or HCl. For MX, DNR, and FITC–R8, the release medium was phosphate buffered saline (PBS) with different pH. In the case of sampling, the release system was centrifuged, after which 1.0 mL of supernatant solution was withdrawn and replaced by the same amount of fresh medium. The released amount of guest molecules was measured by ultraviolet–visible (UV–vis) spectrophotometry.

UV–vis Spectrophotometric Analysis of Formation/Cleavage of Coordination Bonds in Solutions. The formation/cleavage of the coordination bond between metal ions and guest molecules can be characterized by UV–vis spectra. In a typical example, a mixture solution of 0.1 mM of $Cu(ClO_4)_2 \cdot 6H_2O$ and 0.4 mM of

- (32) Schmid, S. L.; Fuchs, R.; Male, P.; Mellman, I. *Cell* **1988**, *52*, 73–83.
 (33) Dautry-Varsat, A.; Ciechanover, A.; Lodish, H. F. *Proc. Natl. Acad. Sci. U.S.A.* **1983**, *80*, 2258–2262.
 (34) Gao, C.; Sakamoto, Y.; Terasaki, O.; Sakamoto, K.; Che, S. *J. Mater. Chem.* **2007**, *17*, 3591–3602.

- (35) Zheng, H.; Gao, C.; Che, S. *Microporous Mesoporous Mater.* **2008**, *116*, 299–307.

propylamine was prepared and the pH was controlled by NaOH or HClO₄ before being diluted to volume. The final solution was spectrophotometrically analyzed in the UV–vis region after reaching a stable state. UV absorbance was measured at wavelengths of 266, 235, 230, and 245 nm when 1,1-dimethylbiguanide, propylamine, ethylene diamine, and diethylene triamine, respectively, was used as the ligand. The change in UV absorbance was normalized for clarity in comparison.

Characterizations. Powder X-ray diffraction (XRD) patterns were recorded on a Rigaku X-ray diffractometer D/MAX-2200/PC equipped with Cu K α radiation (40 kV, 20 mA) at a rate of 1.0°/min over the range of 1°–6° (2 θ). The morphology of AMS nanoparticles was observed via scanning electron microscopy (SEM) (JEOL, Model JSM-7401F) with an accelerating voltage of 1.0 kV. High-resolution transmission electron microscopy (HRTEM) images were taken with a JEOL Model JEM-3010 microscope operating at 300 kV. The nitrogen adsorption/desorption isotherms were measured at –196 °C with a Quantachrome Model Nova 4200E porosimeter. The surface area and primary mesopore volume were calculated by the Brunauer–Emmett–Teller (BET) and α_s -plot methods, respectively. The pore size distribution was calculated by Barrett–Joyner–Halenda (BJH) method, according to the adsorption branch of the isotherm. The solid-state ¹³C MAS NMR spectrum of the AMS nanoparticle was collected on a Varian Model Mercury plus-400 NMR spectrometer at 100 MHz and a sample spinning frequency of 3 kHz. CHN elemental analysis was taken on a Perkin–Elmer Model 2400-II analyzer. The density of aminopropyl groups on the pore surface was estimated by combining the data of elemental analysis and surface area by the following equation:

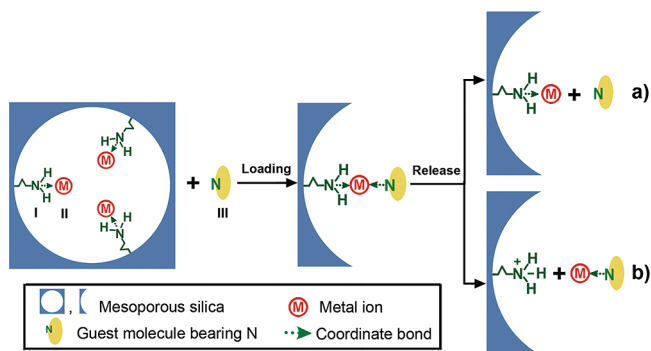
$$\rho = \frac{10^{-18} L N_A}{S}$$

where ρ is the density of aminopropyl (expressed in units of molecule/nm²); L the loading of aminopropyl (in mol/g); N_A Avogadro's constant; and S the specific surface area (in m²/g). X-ray photoelectron spectroscopy (XPS) experiments were carried out on a RBD upgraded Model PHI-5000C ESCA system (Perkin–Elmer) with Mg K α radiation ($h\nu = 1253.6$ eV). Binding energies were calibrated using containment carbon (C(1s) = 284.8 eV). The concentration of guest molecules in solution was measured by a UNICO UV-4802 UV–vis double beam spectrophotometer. Quantitative evaluation of the metal ion in the mesoporous silica was conducted by using an inductively coupled plasma (ICP) emission analysis equipment (IRIS advantage 1000).

Results and Discussion

Strategy for the Coordination-Bonding-Based pH-Responsive System. Scheme 1 shows the strategy for the pH-responsive release system on the basis of coordination bonding in mesopores, which is exemplified by the “metal–N (amino group, guanidine, etc)” bonding. Mesoporous silica^{36,37} nanoparticles with uniformly and separately distributed aminopropyl functional groups (I) on the pore surfaces serve as carriers.^{38–40} Metal ions (II) are readily absorbed

Scheme 1. Schematic Mechanism for the pH-Responsive System Based on Coordination Bonding in Mesopores: (a) Release of Guest Molecules in the Case of Bonding Strength I II > II III and (b) Release of Guest/Metal Complex in the Case of Bonding Strength I II < II III^a



^a I, II, and III represents functional aminopropyl groups, metal ions, and guest molecules, respectively. At a high pH, the functional groups (I) on the pore surface of mesoporous silica nanoparticle carrier are coordinated to metal ions (II), and guest molecules (III) are subsequently bonded to the unsaturated metal ions to form the “host–metal–guest” architecture. When the pH is reduced, guest molecules are detached from the carrier due to the cleavage of either coordination bond.

by host aminopropyl groups to form a “host–metal” coordination bond on the mesopore surface. Subsequently, guest molecules (III) are bonded to the metal ions in the carrier. The presence of a vacancy between these host functional groups caused by their isolated distribution and presence of large mesopores ensures that the metal ion are unsaturated (ignoring the weak metal–H₂O coordination bonding hereafter) and capable of forming coordination bonds with guest molecules. Therefore, mesoporous materials make the “host–metal–guest” architecture possible, in which both the host functional groups and guest molecules are coordinated to metal ion binders. In addition, the host functional groups should be effective for charging of the metal ions, and the “host–guest” (I III) interaction should be weaker than both “host–metal” (I II) and “metal–guest” (II III) interactions. A breakup of either (or both) coordination bond, triggered by a reduction in external pH, leads to the release of guest molecules from the carrier into the surrounding environment. If the “host–metal” bond is stronger than the “metal–guest” bond (I II > II III), the guest molecules will be shed off with metal ions remaining on the carrier when passing through a low-pH region (route a). On the other hand, if the “host–metal” bond is weaker (I II < II III), it will break up when the carrier suffers a decrease in pH, accompanied by a simultaneous release of the guest/metal complex (route b). In the systems that use N as the electron donor (aminopropyl on the mesopore surface, guest compounds containing amino groups or guanidines, etc.), a breakup of the “host–metal” and “metal–guest” coordination bonds may possibly occur, because of the closeness of the bonding strength.

pH Sensitivity of Various Coordination Bonds. The pH sensitivity of various coordination bonds has been evaluated.

(36) Yanagisawa, T.; Shimizu, T.; Kuroda, K.; Kato, C. *Bull. Chem. Soc. Jpn.* **1990**, *63*, 988–992.

(37) Kresge, C. T.; Leonowicz, M. E.; Roth, W. J.; Vartuli, J. C.; Beck, J. S. *Nature* **1992**, *359*, 710–712.

(38) Vallet–Regí, M.; Rámila, A.; del Real, R. P.; Pérez–Pariente, J. *Chem. Mater.* **2001**, *13*, 308–311.

(39) Vallet–Regí, M. *Chem.—Eur. J.* **2006**, *12*, 5934–5943.

(40) Vallet–Regí, M.; Balas, F.; Arcos, D. *Angew. Chem., Int. Ed.* **2007**, *46*, 7548–7558.

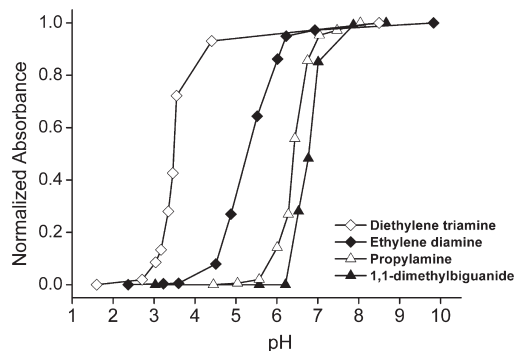


Figure 1. UV absorbance of water solutions comprised of $\text{Cu}(\text{ClO}_4)_2 \cdot 6\text{H}_2\text{O}$ and various types of ligands under different pH conditions.

The formation, cleavage, and pH sensitivity of the coordination bonds between metal ions and different functional groups can be simply tested by UV spectroscopy if the metal–guest compounds have UV absorbance. For a typical example, $\text{Cu}(\text{ClO}_4)_2 \cdot 6\text{H}_2\text{O}$ was chosen as the metal source, and 1,1-dimethylbiguanide, propylamine, ethylene diamine, and diethylene triamine were chosen as model guest compounds bearing guanidine group and different numbers of amino groups, respectively. The relationships between the absorbance and pH of these systems are shown in Figure 1. For each coordination system, the UV absorbance of the combined solution is sharply enhanced with increasing pH in a narrow range and vice versa with decreasing pH, which proves that the coordination bonds can form and break in response to pH variations, because of competitive bonding of guest molecules with metal ions and protons. In addition, the responsive pH onset varies for different compounds, because of variations in the strength of the coordination bond. The responsive pH onset of 1,1-dimethylbiguanide-bearing guanidine groups is higher (pH 6–7), relative to amines, because of the weak affinity to Cu^{2+} , and the responsive pH onsets are systematically decreased in the series of amine, diamine, and triamine, which could be attributed to an increase in the stability of a multidentate chelate complex. Therefore, the responsive pH onset could be well-tuned by controlling the strength of the coordination bonding, which could be achieved by choosing proper functional groups of guest molecules and different types of metal ions. Most significantly, a small pH change (normally unit variation of pH) is sufficient for the formation and cleavage of the coordination bonds demonstrated by an abrupt change in UV absorbance with changing pH, affording designed and precise features of the pH-responsive system.

Characterization of the Aminopropyl-Functionalized AMS Nanoparticle Carrier. Aminopropyl-functionalized anionic–surfactant-templated mesoporous silica (AMS)^{34,35,41–44}

nanoparticles have been considered as outstanding candidates for carriers of this pH-responsive release system. Here, the AMS nanoparticle was synthesized by using C_{18}GluA as the template and APS as the co-structure-directing agent (CSDA). The stoichiometric electrostatic interaction between the anionic headgroup of the surfactant and the amino group of APS produces a uniform distribution and a regular array of amino groups on the pore surface following surfactant arrangement. After the surfactant was removed by extraction, the aminopropyl groups were retained on the pore surface and accounted for the effective charging of metal ions. The distance between the neighboring aminopropyl groups, which is caused by the presence of large mesopores and the isolated and uniform distribution of the aminopropyl groups on the pore surface, ensures the coordination unsaturation of the metal ions to form “metal–guest” coordination bonds.

Figure 2 shows the SEM, TEM, and solid-state ^{13}C NMR of the AMS carrier material bearing aminopropyl host functional groups. The material is composed of monodispersed nanospheres, ~ 100 nm in size as estimated from the SEM image. The TEM image reveals the disordered pore structure, which is also suggested by its XRD pattern showing one single peak within the range of 1° – 6° (2θ) (see Figure 3a-1). The surface area, primary mesopore volume, and pore size are $704 \text{ m}^2/\text{g}$, $0.68 \text{ cm}^3/\text{g}$, and 4.7 nm , respectively, determined by nitrogen adsorption (see Figures 3b-1 and 3c-1). The nitrogen adsorption/desorption isotherm is type IV, which is typical for a porous material, having two obvious capillary condensations at $P/P_0 \approx 0.4$ – 0.7 and $P/P_0 \approx 0.9$, occurring, respectively, in mesopores and cavities produced by packing of the silica spheres. The H2 type hysteresis loop of the isotherm suggests the cage-type mesostructure. After the ion-exchange extraction of the surfactant in ethanolic solution, the presence of the aminopropyl group and its loading density (1.7 mmol/g , ~ 1.5 molecule/ nm^2) have been confirmed by NMR and elemental analysis (C, 7.1 mmol/g ; H, 28.7 mmol/g ; N, 1.7 mmol/g). In contrast to the weak absorption ability of the calcined AMS or extracted MCM-41 to metal ions, these aminopropyl groups impart the AMS material with strong absorption capability of metal ions as can be suggested by the ICP measurement. Wide-angle XRD of the metal-loaded mesoporous materials showed only one broad single peak within the range of 6° – 60° (2θ), because of the amorphous structure of silica, indicating that no crystallization of the metal ion was formed in the mesoporous carriers (see Figure S1 in the Supporting Information).

The stabilities of the AMS nanoparticle carrier and metal-ion-loaded AMS nanoparticles under biologically relevant conditions were confirmed (see Figure 3, as well as Figure S2 and Table S1 in the Supporting Information), which ensures the safe storage and protection of guest molecules before their intended release. After metal ions (Cu^{2+}) or further guest molecules (phenformin) were loaded into the mesoporous silica, the X-ray reflection intensity decreased, because of a reduction in contrast between pores

- (41) Che, S.; Garcia-Bennett, A. E.; Yokoi, T.; Sakamoto, K.; Kunieda, H.; Terasaki, O.; Tatsumi, T. *Nat. Mater.* **2003**, *2*, 801–805.
- (42) Garcia-Bennett, A. E.; Terasaki, O.; Che, S.; Tatsumi, T. *Chem. Mater.* **2004**, *16*, 813–821.
- (43) Gao, C.; Qiu, H.; Zeng, W.; Sakamoto, Y.; Terasaki, O.; Sakamoto, K.; Chen, Q.; Che, S. *Chem. Mater.* **2006**, *18*, 3904–3914.
- (44) Gao, C.; Sakamoto, Y.; Terasaki, O.; Che, S. *Chem.—Eur. J.* **2008**, *14*, 11423–11428.

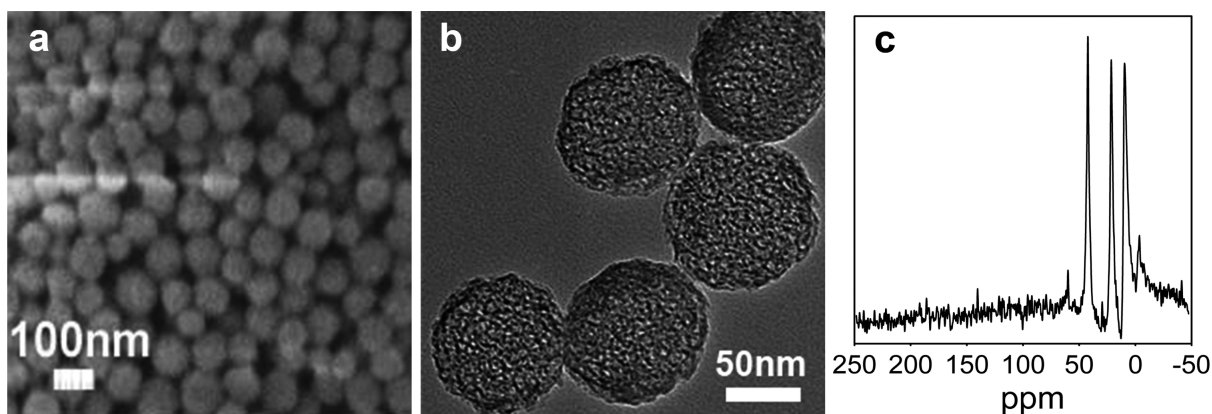


Figure 2. Characterizations of the AMS nanoparticle carrier after removal of surfactant by solvent extraction: (a) SEM image, (b) TEM image, and (c) solid-state ^{13}C NMR spectrum.

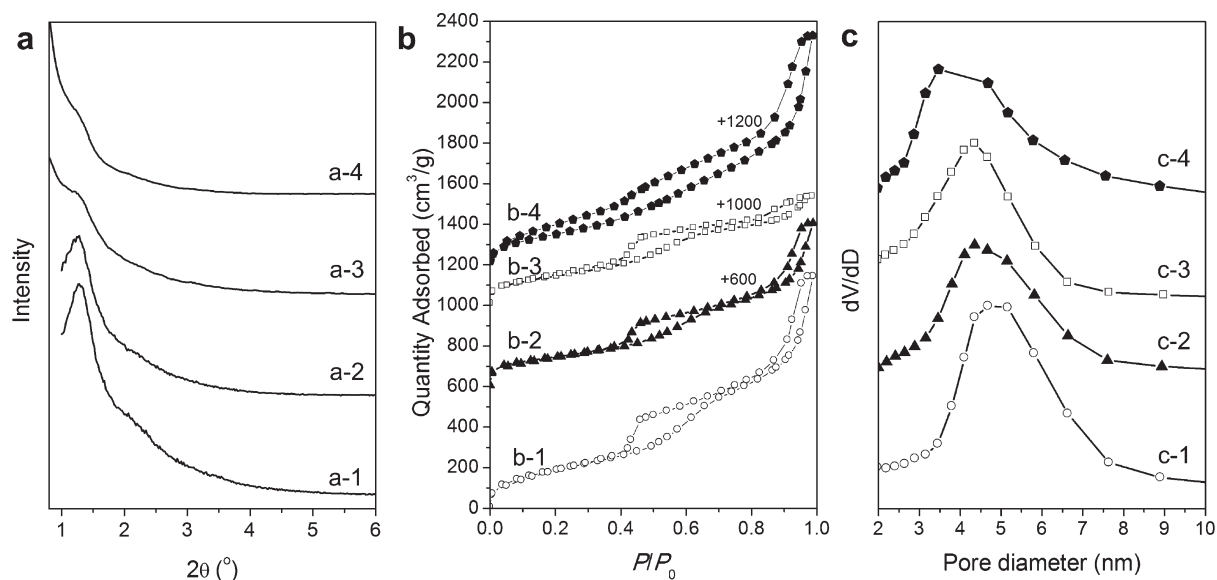


Figure 3. (a) XRD, (b) nitrogen adsorption/desorption isotherms, and (c) pore size distributions of the AMS nanoparticles in the preparation of the drug (phenformin) delivery system and in the drug release. The materials are AMS nanoparticles after the removal of surfactant (denoted as a-1, b-1, and c-1), AMS nanoparticles with Cu^{2+} loading (denoted as a-2, b-2, and c-2), AMS nanoparticle after loading of Cu^{2+} and phenformin (denoted as a-3, b-3, and c-3), and AMS nanoparticle after treatment at pH 7.0 for 6 h (denoted as a-4, b-4, and c-4).

and walls. The nitrogen adsorption/desorption isotherms of the mesoporous silica carriers were close to that of the pristine one, confirming the intact mesopores. The primary mesopore volume and pore diameter slightly decreased, which could be reasonably attributed to the adsorption of metal ions and guest molecules. After the material was treated in aqueous solution at pH 7.0 for 6 h, the deterioration in XRD pattern and a more dramatic reduction in the pore size of the mesoporous silica have been observed, indicating a decrease in the mesoscopic ordering of the AMS nanoparticles. Nevertheless, the nitrogen adsorption/desorption isotherms still showed type IV features, having two distinct hysteresis loops at the same relative pressures as those of the pristine sample, although the isotherm was not well reversible. Besides, the high porosity (surface area and pore volume) was detected by nitrogen adsorption, which confirmed that the mesopore system has been retained.

pH-Responsive Release of Guest Molecules from Different Coordination Bonding Systems. Figure 4 shows the release of some typical N-coordinating guest compounds

(*o*-phenylenediamine bearing a diamine and phenformin bearing a guanidine group) via different “ NH_2 –metal–guest” coordination bonding using AMS nanoparticle as a carrier, to demonstrate the responsiveness of the system to pH variations and its designability. The release profiles were obtained at different pH ranging from pH 8.0 to pH 1.2.

As shown in Figure 4 b, when phenformin was chosen as the guest molecule and Cu^{2+} as the coordinating center in the carrier (Cu^{2+} , 1.1 mmol/g; Cu^{2+} /aminopropyl, 0.65), the responsive pH onset was determined to be 6.0, as the release percentages were $\sim 50\%$ and $\sim 60\%$ at pH 6.0 and pH 5.0, respectively, and only $\sim 5\%$ at pH 7.0. The dramatic release of guest molecules was caused by a preferential cleavage of “ Cu^{2+} –guanidine” coordination bond at pH 6.0 and pH 5.0, derived from the XPS analysis (see Figure 5), which is consistent with the sequence of coordination bonding strength indicated by Figure 1.

When another guest molecule, *o*-phenylenediamine, was used in the pH-responsive system with Cu^{2+} as the

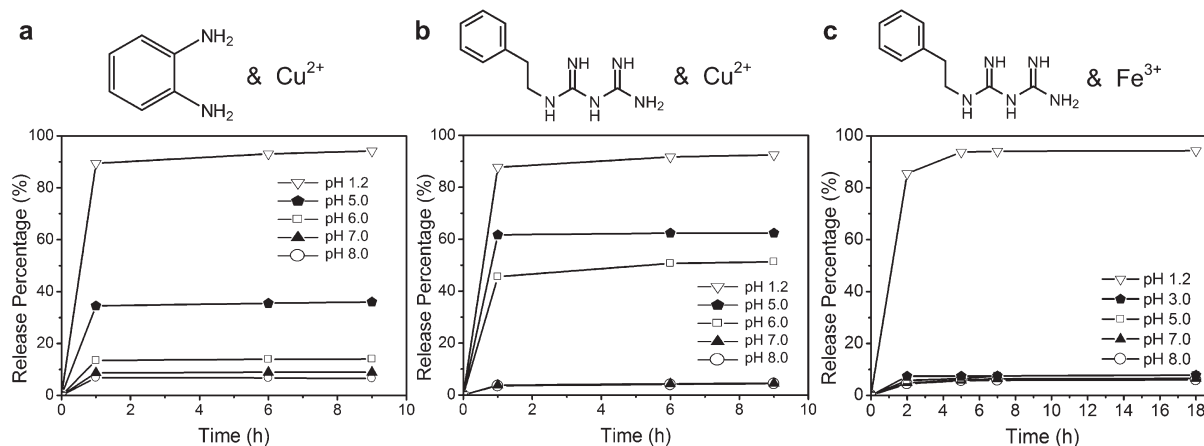


Figure 4. pH-responsive release of guest molecules from different “NH₂–metal–guest” coordination bonding systems. The guest and metal ions are (a) *o*-phenylenediamine and Cu²⁺, (b) phenformin and Cu²⁺, and (c) phenformin and Fe³⁺.

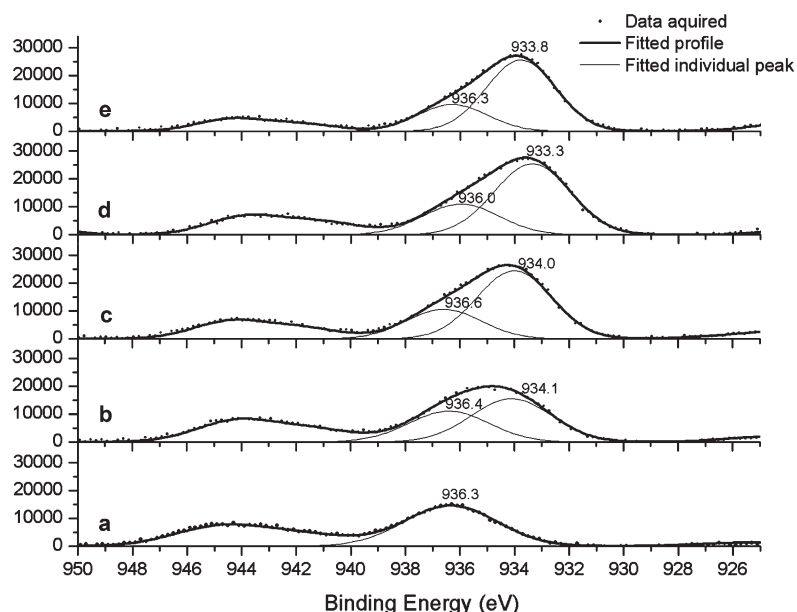


Figure 5. Cu(2p_{3/2}) XPS spectra of the Cu²⁺-loaded AMS nanoparticle in the process of absorption and release of phenformin from the “NH₂–Cu²⁺–guanidine” system. The materials are AMS nanoparticles after absorption of Cu²⁺ (a) in ethanol (EtOH), (b) after further treatment with water at pH 7.0, (c) after absorption of phenformin from a water solution at pH 7.0, (d) after release at pH 6.0, or (e) after release at pH 5.0.

coordinating center in the carrier (Cu²⁺, 0.98 mmol/g; Cu²⁺/aminopropyl, 0.58), the responsive pH onset was decreased to 5.0, because the release percentages were ~35% at pH 5.0 and only ~8% at pH 7.0 (see Figure 4a). This reduction in responsive pH onset could be attributed to the higher strength of the “Cu²⁺–diamine” coordination bond than the “Cu²⁺–guanidine” bond, which is consistent with the result shown in Figure 1. The different bonding ability of the guest amine species to metal ions (Lewis acid), from another perspective, could be also suggested by its p*K*_a value, which reflects its bonding affinity to H⁺. The p*K*_a value of *o*-phenylenediamine (~4.4) is higher than that of phenformin (~2.7), which indicates the stronger bonding strength of *o*-phenylenediamine to H⁺ and probably to other Lewis acids (such as metal ions), giving rise to the reduced responsive pH onset when applied in our pH-responsive system. Therefore, the responsive pH onset of a pH-responsive system could be

well-tuned by controlling the properties of the functional groups of the guest molecule.

The responsive pH onset of the system could be further tuned by varying the type of the coordinating centers. Different metal ions possess different bonding affinities to both host functional groups and guest molecules due to the diverse electron configurations and the nature of the metal ions. As shown in Figure 4c, when Fe³⁺ was used in the pH-responsive system for the release of phenformin (Fe³⁺, 0.24 mmol/g; Fe³⁺/aminopropyl, 0.14), the responsive pH onset was dramatically reduced, compared with the system using Cu²⁺ as the coordinating center. Almost zero release of phenformin was observed if the pH of the release medium was higher than 3.0, and the complete release was observed at pH 1.2. Therefore, the responsive pH onset is in the range of pH 1.2–3.0 for this system. This phenomenon indicates that a designated responsivity could be well achieved by carefully choosing

the type of the metal ions in the construction of the pH-responsive system.

A Study of the Coordination Bonding Mechanism by XPS. The coordination bonding mechanism of the pH-responsive system can be confirmed by monitoring the valence status of the metal ions via XPS. Figure 5 shows the Cu(2p_{3/2}) XPS spectra of the materials at different stages of absorption and release (see the areas and area ratios of the XPS peaks in Table S2 in the Supporting Information), taking “NH₂–Cu²⁺–guanidine” system for example. After loading Cu²⁺ into the AMS nanoparticles in EtOH, a single peak centered at 936 eV was observed, indicating that the Cu²⁺ ions were in the single form of a low coordination state bonded to aminopropyl groups on the carrier. The satellite peak at 944 eV confirms the presence of Cu²⁺ in the carrier. When the Cu²⁺-loaded AMS nanoparticle was placed into an aqueous solution in pH 7.0, the XPS peak at 936 eV decreases in area and another peak appears, centered at a lower binding energy of 934 eV, which reveals an increase in the electron density of Cu²⁺ and, therefore, an increase in the coordination number of Cu²⁺; i.e., both the aminopropyl groups and water molecules were coordinated to Cu²⁺ binders. When the guest molecules (phenformin) were further absorbed by the material in an aqueous solution at pH 7.0, the XPS peak at 934 eV gets dramatically larger and the area ratio of the two peaks rises from 1.4 to 2.3, indicating a more significant formation of coordination bonds of Cu²⁺ in the AMS nanoparticle carrier. After the material was immersed in an aqueous environment at pH 6.0 and pH 5.0, ~50% and ~60% of the guest molecules have been released, respectively; however, the XPS peaks of the material are close to those before release in both the area and the area ratio of the two peaks, which excludes the dramatic cleavage of coordination bonds between aminopropyl groups and metal ions. Therefore, the release of guest molecules at pH 6.0 and 5.0, to a high extent, can be attributed to a breakup of the coordination bonds between metal ions and guest molecules, after which the vacant binding sites of Cu²⁺ were reoccupied by water molecules, compensating for the decrease in peak area at 934 eV.

The release mechanism in the “NH₂–Cu²⁺–guanidine” system could be supported by ICP measurements (see Table S3 in the Supporting Information). The loading density of Cu²⁺ in the mesoporous silica remains high, with slight fluctuations after treatment in pH 7, 6, and 5, which is close to the loading amount in the as-prepared sample. It indicates that the metal ions are mostly coordinated to the aminopropyl in the mesopores during the drug release, and the significant drug release could be reasonably ascribed to the cleavage of the “Cu²⁺–guanidine” coordination bond, depending on the relative bonding strength.

pH-Responsive Release of Anticancer Drugs Bearing Binding Sites. As is well-known, the extracellular pH in tumors (pH 5.7–6.8) is lower than the physiological conditions (pH 7.4);³¹ therefore, the pH-responsive release system might be applied in anticancer therapies.

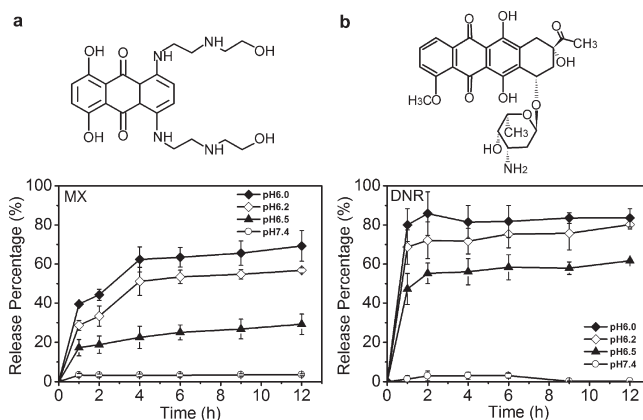


Figure 6. pH-responsive release of anticancer drugs (a) mitoxantrone (MX) and (b) daunorubicin hydrochloride (DNR) from the “NH₂–Cu²⁺–guest” coordination bonding systems.

In the case of the anticancer drug bearing binding groups, a direct coordination bonding of the drug to the metal ions in the AMS nanoparticle carriers could be employed for the pH-responsive uptake and release. Two typical anticancer drugs, mitoxantrone (MX) and daunorubicin hydrochloride (DNR), were used directly in this pH-responsive system, on the basis of “NH₂–Cu²⁺–MX/DNR” coordination bonding. There are amino, carbonyl, and hydroxyl groups in a molecule of MX, hydroxyl, carbonyl, and amino groups in a molecule of DNR, which serve as binding sites to Cu²⁺ ions in the mesoporous silica carrier. The drug-loading capacities of these carriers (Cu²⁺, 0.69 mmol/g; Cu²⁺/aminopropyl, 0.40) reach as high as 53 and 46 mg/g for MX and DNR, respectively, in our experiments. The release profiles of MX and DNR under the physiological condition (pH 7.4) and slightly acidic conditions (pH 6.5, 6.2, 6.0, and 5.0) are presented in Figure 6. No significant release of the anticancer drugs from the AMS nanoparticle carriers has been observed under the physiological conditions; however, under mildly acidic conditions, drugs are released in significant amounts from the carrier into the external environment, i.e., 29% and 62% release, respectively, at pH 6.5 and 69% and 84% release, respectively, at pH 6.0, in 12 h, for MX and DNR. The release amount of drugs is proportional to the pH reduction; i.e., lower pH triggers the release of a larger amount of drugs, because of less competitive formation of coordination bonds between metal ions and anticancer drugs. It implies the direct applicability of the anticancer drugs that bear functional groups in this pH-responsive system and the potential use of this system in anticancer therapies.

Vector-Aided pH-Responsive Release of Drugs without Significant Binding Capabilities. In the case of a guest compound that has a weak binding affinity to metal ions, a vector that possesses abundant binding sites could be employed to conjugate to the guest molecule and endow it with the capability to be charged into the carrier and released in response to external pH variations (see the scheme shown in Figure 7a). Here, fluorescein isothiocyanate (FITC) was chosen as the model guest compound, and octaarginine (R8) was employed as a vector, which was

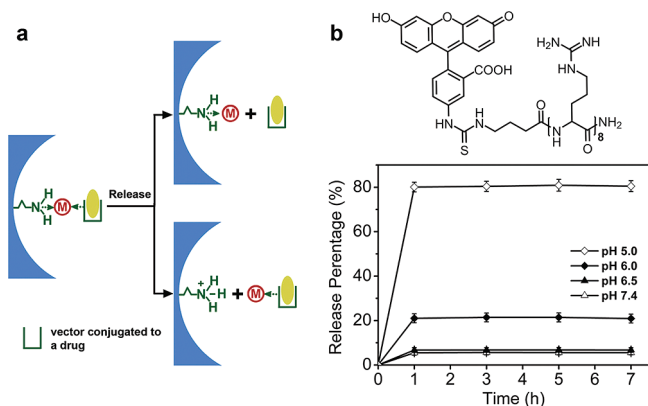


Figure 7. Vector-aided pH-responsive system for drugs without significant binding capabilities: (a) a scheme for the construction and drug release of the vector-aided pH-responsive system and (b) pH-responsive release of the FITC-R8 from the “NH₂–Zn²⁺–R8” coordination bonding system.

bonded to the model drug via covalent bond. The eight guanidine groups of the R8 vector serve as the binding sites to the metal ions (Zn²⁺), which are bonded on the inner surface of the AMS nanoparticle, forming “NH₂–Zn²⁺–R8” coordination architecture. The loading amount of the FITC–R8 conjugate in the carrier (Zn²⁺, 0.99 mmol/g; Zn²⁺/aminopropyl, 0.58) is as high as 73 mg/g. The release of the FITC–R8 conjugates from the mesoporous silica carrier was conducted, and the profiles are shown in Figure 7b. It can be inferred that the responsive pH onset for this system is ~6.0, because a negligible amount of FITC–R8 is detected to be released at pH 7.4 and 6.5 and significant release is observed at pH 6.0 (above 20%) and lower (80% at pH 5.0). It suggests that utilizing a vector is a feasible solution for coordinately inert drugs to respond to pH variations. This system might be useful for drug delivery when endocytosis is involved as the pH value in endosomes is as low as 5.5.³² In addition, R8 proved to have enhanced penetration capability through biomembranes,⁴⁵ which may show advantages in therapeutic applications.

In this work, we have demonstrated a mesoporous-silica-based pH-responsive release system, using N as the electron donors on both sides of the “host–metal–guest” architecture, which is believed to break up under close pH conditions and thus show better responsiveness. Other systems are being exploited and will be reported shortly. In this work, AMS nanoparticle material was employed as the carrier of the pH-responsive release system. The functionalization of mesoporous silica could be also achieved by co-condensation and post-graft methods. Using these carrier materials, a pH-responsive release of guest molecules could also be achieved by carefully

choosing the experiment conditions (to be addressed in future work). Obviously, the distribution of the functional groups in these materials is inhomogeneous, which adds a complication to the pH-responsive release system. The pH-responsive release systems based on the coordination bond show low cytotoxicity (see Figure S3 in the Supporting Information). When Zn²⁺ was chosen as the coordinating center, the relative viability of cells are as high as 94% and 90% in the “Zn²⁺–phenformin” and “Zn²⁺–FITC-R8” systems, respectively. For better biocompatibility of the system, the use of nontoxic metal ions (e.g., Zn²⁺) and the construction of strong “host–metal” coordination bonds are highly valued and will be better explored. Other carriers, which could be either organic or inorganic, in the form of hydrogels, micelles, nanoparticles, or porous solids, etc., are also theoretically eligible for the loading of metal ions and guest molecules in the pH-responsive system.

Conclusion

In conclusion, we have demonstrated the feasibility of constructing a pH-responsive release system based on coordination bonding in mesopores via “host–metal–guest” architecture. The formation and cleavage of coordination bonds have proved to be sensitive to pH variations. Aminopropyl-functionalized AMS nanoparticle material is used for hosting metal ion and ensuring its coordination unsaturation for further interaction with guest molecules. Successful pH-responsive release of guest molecules has been observed, and prominently typical anticancer drugs have been released under weakly acidic conditions (pH 5–6.5). Besides, a vector has been designed to endow coordinately inert drugs with pH-responsive properties.

To the best of our knowledge, this is the first report of a pH-responsive system based on coordination bonding in mesopores. Our system opens up a powerful route and new opportunities for pH-responsive drug delivery applications, especially for anticancer therapy. Potentially, this pH-responsive system might be used in broader applications, e.g., gene transfection therapy.

Acknowledgment. We acknowledge the support of the National Natural Science Foundation of China (Grant No. 20890121 and 20821140537), the 973 Project (No. 2009-CB930403), and Grand New Drug Development Program (No. 2009ZX09310-007) of China.

Supporting Information Available: Preparation of anionic surfactant C₁₈GluA; porous properties of the AMS nanoparticles in the preparation of the drug delivery system and in the drug release; the area and area ratios of the Cu (2p_{3/2}) XPS peaks centered at 934 and 936 eV; density of Cu²⁺ in the mesoporous silica during drug loading and release. This information is available free of charge via the Internet at <http://pubs.acs.org/>.

(45) Rothbard, J. B.; Garlington, S.; Lin, Q.; Kirschberg, T.; Kreider, E.; McGrane, P. L.; Wender, P. A.; Khavari, P. A. *Nature Med.* **2000**, *6*, 1253–1257.